THIN-FILM LIQUID CRYSTAL INDICATORS OF TEMPERATURE AND SHEAR STRESSES ON THE MODEL SURFACE

G.M. ZHARKOVA, V.N. KOVRIZHINA

[1]Khristianovich Institute of Theoretical and Applied Mechanics, Novosibirsk, 630090, Russia

Zharkova G.M.: Tel.: +83833303896; Email: zharkova@itam.nsc.ru

KEYWORDS:

Main subjects: flow visualization**,** temperature measurements
Fluid: subsonic flows, high speed flows
Visualization method(s): shear- and temperature sensitive liquid crystals
Other keywords: laminar-to-turbulent transition, separation

INTRODUCTION. At the moment, together with the methods of measurement of local flow parameters on the model surface (temperature, shear stresses), the methods of panoramic visualization and measurement of these parameters are developing. In addition to the infrared thermometry (IRT), the methods based on optical properties of thin-film coatings can be also referred here. These are temperature sensitive paints (TSP) and phosphor thermography [1], shear stress sensitive films (S3F) [2], global interferometer skin friction meter (GISF) [3], and the methods using thermo-optical and mechano-optical effects in liquid crystals: liquid crystal thermography (LCT) and shear sensitive liquid crystals SSLC [4 – 6].

Application of LC coatings for flow diagnostics begins from the pioneer work of Klein and Margozzi [4 – 5]. The possibility to obtain panoramic visual information drew attention of aerodynamicists in many research centers. Potential of cholesteric liquid crystals in aerodynamic experiments is related with the sensitivity of their optical properties to temperature and shear. There are different requirements to the indicators for temperature and shear stress diagnostics. To measure the temperature and heat fluxes, liquid crystals must be protected from the mechanical shear influence. For the purpose thermoindicator films capsulated into a polymer matrix were created in ITAM; they are temperature sensitive but shear insensitive. They were tested within the wide range of experimental conditions, and gave new experimental data [7 – 9]. The panoramic temperature distribution over the aerodynamic model surface permits to determine the areas of transition of laminar flow into the turbulent, separation and reattachment regions, as well as the effects of shock/boundary layer interaction [10]. One condition of the application of such indicators is that the model must be fabricated of a material with low heat conductivity. When the flow around a metal model is studied, the error in temperature field measurement may be considerable due to heat spreading. Thus, in case of visualization of the flow peculiarities on a metal model surface, it is more preferable to use the optical effect which occurs when the LC layer shifts under the action of an air flow. Shear stress is more sensitive to varying character of the near-wall flow than the temperature. Optical properties of liquid crystals should be insensitive to the temperature in this case .

This paper presents some results in the development and research of the properties of thin-film indicators based on cholesteric liquid crystals; as well as examples of application of these indicators for the panoramic diagnostics of the near-wall flows.

1. CHARACTERISTICS OF LC INDICATORS OF TEMPERATURE AND SHEAR STRESSES

Within a certain temperature range ΔT and at a certain molecules orientation in the layer, the cholesteric LCs (ChLCs) have the properties of selective light reflection. The reason lies in the lamellar helix structure of these substances (Fig. 1). Most commonly, non-oriented cholesterics form a confocal texture [11] (Fig. 1a). It consists of separated and connected to each other domains called as confocal domains, and features the intensive light scattering. Under the influence of external factors, LC molecules re-orient which results in a variety of optical effects in LC films. In particular, when the cholesteric LC helix axis is perpendicular to the surface (Fig. 1b), the texture of LCs is called planar or Granjean texture. Such texture selectively reflect light with maximum of wavelength depending on temperature and/or shear stress magnitude. In aerodynamics, normally the second LC texture and its property is used.

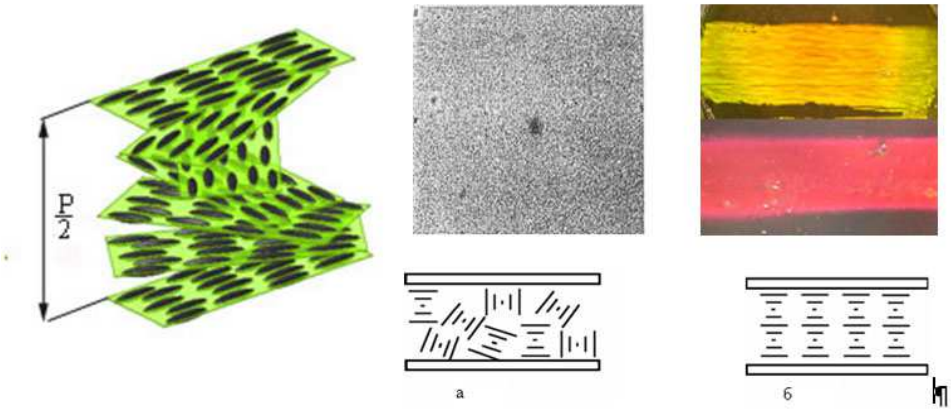

Fig.1. ChLCs structure and textures: confocal (a), planar (b).

Among most important characteristics of the LC indicators there are: working temperature range of selective reflection ΔT_{LC}; thermal sensitivity $\Delta\lambda/\Delta T$; angular dependence of reflection spectra. For the LC indicators of the shear stresses: working temperature range of selective reflection ΔT; $\lambda(\tau = 0)$, the length of selective reflection wave when the shear stresses are absent; it is wished that this length corresponds to red color of coating; working range or threshold levels of the shear stresses $\Delta\tau=(\tau_{min}\div\tau_{max})$, which are governed by viscous-elastic properties $\Delta\lambda = \lambda(\tau_{min})\div\lambda(\tau_{max})$; shear sensitivity $\Delta\lambda/\Delta\tau$; adhesion to the model material surface. Above characteristics depend on the LC mixture composition. There are the mixtures which have the dynamic temperature range ΔT_{LC} from 0.02 to 50° in the temperature area from -20 to 150°C.

Besides, for the panoramic visualization by LCs, the possibility of quantitative expression of color difference, the color contrast is of big practical importance. Hence, aside for the spectral characteristics, colorimetric ones are also used for analysis [12]. To do this, the color response of the LC to the input signal is registered. The obtained color image is digitized and transformed into a color coordinates R(red), G(green), B(blue), and then into the colorimetric system which fits better for the measurements. In our tasks, the most common color coordinate system is the HSI system (hue, saturation, intensity). In this system, the hue shows the angular position (red-based polar angle). The unit of hue measurement is radians or degrees, and the range of 2π (or 360°) corresponds to 255 gradations. Qualitatively, the H value varies approximately inversely to the wave length. Such a colorimetric characteristic as the color gamut – the area in the color chart, or the volume in the color space [12] is a non-conventional but useful in aerodynamic applications property which has come from optic electronics. Usually, this part of the color chart (color space) covers all colors which can be reproduced with any color process. In our case, it is the color response of the LC indicator to the parameters (temperature, shear stress) variation. The usefulness of this approach is that this parameter permits to show clearly the degree of color difference of various indicators and to select proper ones.

As for dynamic characteristics, repetitive experiments have shown that the LC thermal indicators enable to detect only low-frequency (<30 Hz) temperature oscillations, so it is possible to register the variation of average level of temperature and heat fluxes alone. The response time of pure LC to the shear is one order shorter and depends on the indicator mixture viscosity, but these indicators either do not permit to visualize high-frequency pulsations.

3. DIFFERENT FORMS OF LC INDICATORS AND CONDITIONS OF THEIR APPLICATION

In the experiment LCs undergo simultaneous action of the non-stationary temperature, pressure, and shear stresses. As for the variation of the optical properties of ChLCs under the static pressure action, [13], in most thermal aerodynamic experiments, this variation is neglected because of the effect nullity. Thus, the cholesteric helix pitch p depends on the temperature and mechanical shift (shear stress) $p = P(T, \tau)$, and, if the length of the selective reflection wave λ_o appears to be in the visible spectrum, the sample will look colored. To measure the shear stresses, pure LC are utilized. The temperature effect can be excluded or minimized by the LC mixture design. To measure the temperature, the polymer-encapsulated CLC (LC composites) are used. The shape of used LC materials and their brief description are given in the Table. Foreign researchers usually utilize commercial LC mixtures. In our experiments, the LC indicators made in ITAM SB RAS were used. In order to increase the measurement accuracy at the low flow speed (and small temperature drop on the studied surface), the mixtures with the narrow range of selective reflection ($\Delta T\approx3\div5$°C) are used, whereas at hypersonic speeds, the range is wider

(ΔT≈5÷20°C). LC mixture composition is designed in accordance with the expected surface temperature gradient. The maximum surface temperature gradient associated with the varying flow-around regime $\Delta T_w = (T_{w\,turb} - T_{w\,lam})$ for the thermally-insulated wall at various Mach numbers M can be evaluated with the equation: $\Delta T_w = \frac{(\gamma-1)(r_{turb}-r_{lam})}{2} T_\infty M^2 \approx 0.008 M^2 T_\infty$

Table 1

LC forms	Description		
LC composites: cholesteric LCs encapsulated in a polymer matrix (film)	Sensitive to temperature, but insensitive to the shear stresses τ (the width of selective reflection range ΔT=3÷30°C).	Shift of the selective reflection wave length under the influence of temperature $\Delta\lambda_T(\Delta T)$ to 300 nm And under shear stress $\Delta\lambda_\tau(\Delta\tau)$<2÷5 nm	Multicolor, for the models made of a low heat-conductive material
Pure ChLCs, their mixtures and mixtures of ChLCs and chiral (twisted) nematic LCs	1. Temperature and shear sensitive. 2. Temperature insensitive but shear sensitive (Δτ≈1÷1000 Pa [15])	$\Delta\lambda_T(\Delta T)$ to 300 nm $\Delta\lambda_\tau(\Delta\tau)$ to 40 nm $\Delta T \to \infty$ $\Delta\lambda_T(\Delta T)$ < 2÷5 nm $\Delta\lambda_\tau(\Delta\tau)$ to 30÷40 nm	Multicolor, for the models with low heat conductivity One-color gradation, or multicolor, for the models made of metal and/or with low heat conductivity

4. ANGULAR DEPENDENCE OF SELECTIVE REFLECTION AND ITS ROLE

It is known that cholesterics are characterized by the angular dependence of selective reflection spectrum. For samples of pure LCs, basing on the Bragg's condition and laws of light reflection, the formulas have been obtained which bind the length of maximum selective reflection wave λ_0 and angles of incidence (φ_n) and observation (φ_o) in the vertical plane [13,14].

$$\lambda_0 = P\bar{n}\cos\frac{1}{2}\left[\arcsin\left(\frac{\sin\varphi_n}{\bar{n}}\right) + \arcsin\left(\frac{\sin\varphi_0}{n}\right)\right]$$

Fig. 2 shows the example of the experimental angular dependence of the selective reflection for the pure thermoindicator mixture. It is evident that as the observation angle θ varies in the vertical plane from 8 to 58° , the selective reflection wave length shifts toward the short-wave part of the visible spectrum to $\Delta\lambda(\theta) \approx 150$ nm. Encapsulation into the polymer protects from the mechanical shift action and simultaneously decreases the angular dependence. As the angles between the light source and camera below 10÷15 degrees, the angular dependence of the LC composites can be treated as negligibly small. Coinciding axes of the light source and registering camera make this dependence null. It is important that this property – the angular dependence of the selective reflection for the LC thermoindicators – is a disadvantage in the case of aerodynamic experiment; today, this disadvantage restricts the application of these indicators in small models with high surface curvature, whereas it is an advantage in the case of LC-indicators of the shear stresses τ because it enables to detect the direction of vector τ [15].

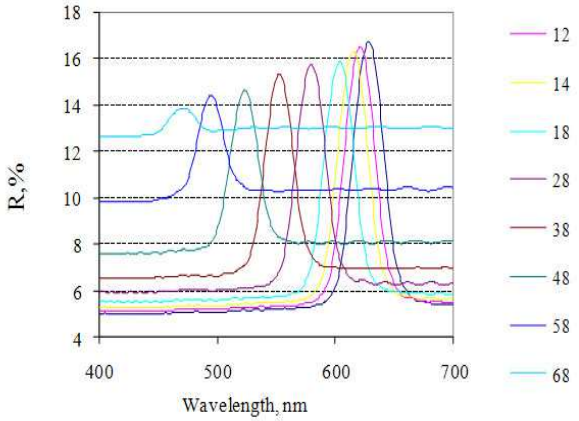

Fig. 2. Angular dependence of the spectra of the selective reflection of the pure LC at normal lighting and T = 23C.

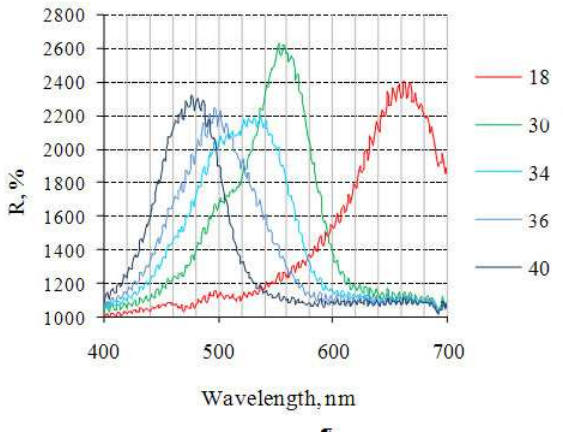

Fig. 3. The blue shift of the maximum wave length of the total (diffusive + mirror) reflection during the heating of the LC composite. Measurement geometry D/8:e.

5. TEMPERATURE AND SHEAR STRESS EFFECT ON SPECTRAL AND COLOR RESPONSE

It has been established that for most low-molecular ChLCs and their mixtures, the maximum of the selective reflection is shifted toward the short-wave part of the spectrum (the blue shift) with temperature and shear stress increasing (Fig. 2 – 4). Thus the resulting action is summed up. The shift resulting from the shear stress variation is considerably smaller than the shift caused by the temperature variation (see Table 1).

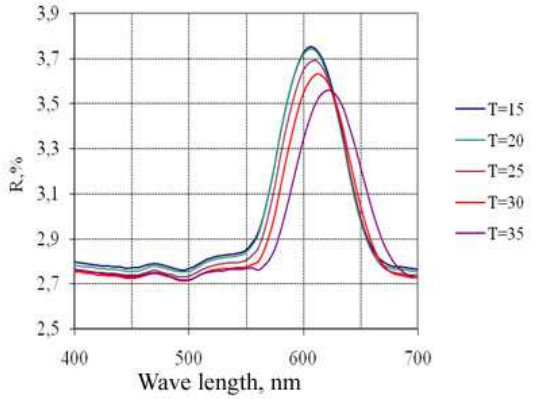

Fig. 4. An example of the weak temperature dependence (0.5 nm/degrees) of the selective reflection spectrum for a triple mixture of pure ChLCs.

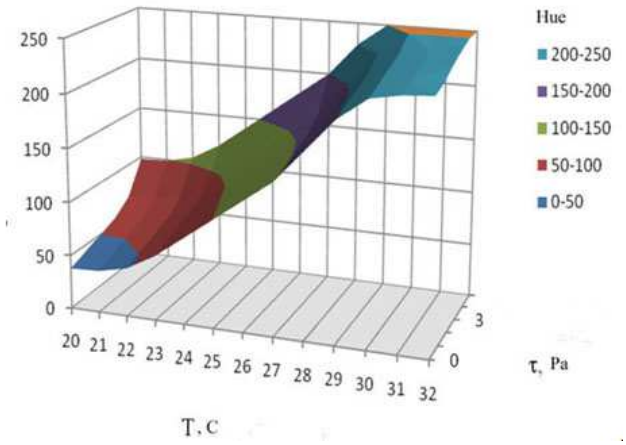

Fig. 5. Dependence of the colorimetric coordinate Hue on the temperature and shear stress. Observation angles θ = 15 and azimuth φ = 0 degrees (streamwise observation).

For the panoramic measurements by the LC-indicators, their color response hue to the input signal is registered. Experimental study of the hue dependence both on the temperature H(T) and on the shear stresses H(τ) has revealed that there is a monotonic dependence between these parameters in the temperature region of the selective reflection. It may be used as calibration to obtain quantitative data. The weak point of the method is the necessity to perform the calibration in real experimental conditions (in situ), which is sometimes impossible. Fig. 5 presents the example of the two-parametric calibration H(T, τ) for the pure ChLCs mixture with the fixed observation angles, at the normal lighting. At the color measurement, the accuracy depends on the lighting and camera adjustment. In the general case it is assumed that the color registered by the camera sensor will differ from the true one but can be corrected with linear correction like $(R_cG_cB_c)^T = M\,(R_dG_dB_d)^T$. Here, vectors from the right and left side of the equation contain the measured and corrected color coordinates, respectively. To calibrate the video camera, for example, a set of color plates with known chromatic coordinates can be utilized. M is a matrix of

color correction, its dimension is 3x3, it was found after the correction equation solution and is then used for the measurement results correction [16].

6. VISUALIZATION AND MEASUREMENT OF TEMPERATURE FIELDS AND HEAT FLUXES

In the real experiment, various boundary conditions may be realized or artificially created on the model surface. These conditions govern the mathematical model design and the algorithms digital processing and calculation of the heat fluxes toward the studied surface. At subsonic flow speeds, the second-kind boundary conditions occur on the surface of the flowed model (known heat flux density $\dot{q}$ on the surface). To create them artificially, the adiabatic model ($\dot{q}$=0) is used, or the model with the ohmic heating ($\dot{q}$=const)). In such models, similarly colored surface sections will correlate with the similar heat flux densities, which simplifies significantly the experimental results interpretation and increases the experiment clearness. In the models made of high heat-conductive materials, it is needed to correct the error caused by the heat spreading, or to put a heat-insulating coating. The latter can be done of a black paint layer necessary to observe the selective reflection. In high-speed hypersonic wind tunnels, the shape of the input thermal impulse may be different (step-like, exponential, with a linear section, etc.). In the case of step action, usually the analytical solution of the heat-conductivity equation for a semi-infinite body is used. Table 2 presents some methods and formulas utilized to determine the heat-flux densities with the aid of LC (one- dimensional task).

Table 2

Wind tunnels (ITAM SB RAS)	Application conditions	Calculation formulas
Subsonic wind tunnels AT-324, MT-324	Adiabatic model ($\dot{q}$=0) or model with ohmic heating ($\dot{q}$=const).	Stationary method Heat transfer coefficient is calculated as $\alpha(x,y)= q/(T_{LC} - T_{gas})$
Hypersonic short duration wind tunnels AT-303, AT-327	At $T_{cr}/T_r << 1$ or $\Delta T = (T_{cr}-T_{ini}) << (T_r - T_{ini})$ 2nd kind of boundary condition q(x,y) = const step impulse	Transient method Heat flux density in the point was defined as follows: $q(t)=\frac{\sqrt{\pi\cdot\rho\cdot c\cdot\lambda}\cdot(T_w(t)-T(t_0))}{2\sqrt{(t-t_0)}}$ Here, t and t_0 are two consequent time instants. $(\rho c\lambda)^{0,5}$ [Вт·м^2·К$^{-1}$·с$^{-0,5}$] is the thermal product of the model material.
Hypersonic long duration wind tunnel AT-326	3rd kind of boundary conditions h(x,y) = const step heat impulse semi-infinite body no heat overflows on the surface	Transient method Heat transfer coefficient $h(x,t)=\frac{\beta\varepsilon}{\sqrt{(t-to)}}$ is determined by the dimensionless excessive temperature, $\theta(\beta)=\frac{T_w-T_i}{T_r-T_i}=1-e^{\beta^2}\cdot erfc(\beta)$, where $erfc(\beta)=1-erf(\beta)=1-\frac{2}{\sqrt{\pi}}\int_0^{\beta}e^{-u^2}du$ $\beta = Bi\sqrt{Fo}=\frac{h}{\lambda}\sqrt{a(t-t_o)}$ Heat flux density $q(x,t)=h(x)[T_r-T_w(x,t)]$,$T_w$ – surface temperature,Tr – recovery temperature, Ti – initial model temperature.

Examples of temperature field visualization at the hypersonic flow around the model. In the hypersonic short duration wind tunnels, the measurement time may be from units to dozens milliseconds. Flow visualization and study of heat transfer are the most topical tasks. Measurement of the heat load in the complex interference region, wherein the measurement with the needed spatial resolution is problematic even for simple models, is of special interest.

Visualization of the step effect on the temperature field at Mach number M = 14. Fig. 6 shows the example of temperature distribution visualization on a conic section of the surface of a reentry ballistic vehicle at the zero angle of attack (the model is made of a thermal-insulating material) in the hot-shot wind tunnel AT-303 ITAM SB RAS. In the point of head part and conic part joint, there is a step of 2 mm height. The details of the experiment are described in [17]. It is seen that the red region behind the step is of lower temperature, it is followed by the hotter region of flow reattachment. The regions with different flow structures are clearly seen on the deflected flap of the vehicle, too.

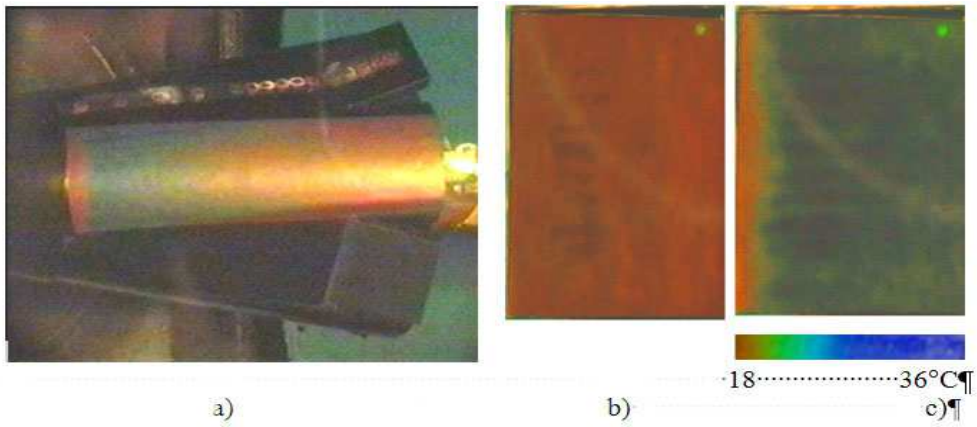

Fig. 6. LC visualization of temperature distribution over the surface of the reentry ballistic vehicle: (a) behind the 2-mm step; (b) and (c) flow reattachment on the flap surface at two time instants.

Temperature field visualization on the blunt cone model at M = 10.9 in the conditions of AT-303. In Fig. 7 LC-visualization of the temperature field on the blunt cone surface at the zero angle of attack is presented. The registration was done at three recording speed (25, 60, and 125 frames per second). The light source power was increased from 500 to 3,000 W with increasing the recording speed.

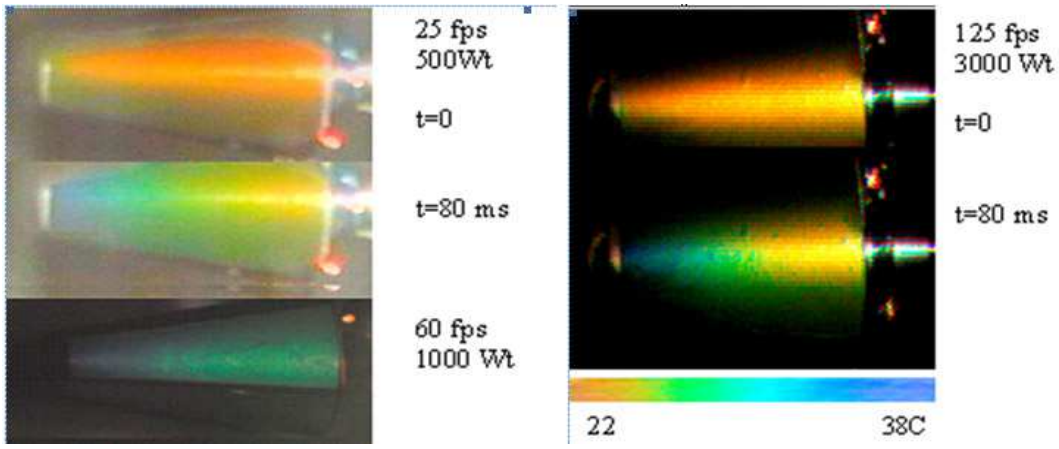

Fig. 7. LC temperature field visualization on the blunt cone surface at the zero angle of attack at three shooting speeds (25, 60, and 125 fps).

Visualization of sharp cone heating at M = 10.9 in the conditions of AT-303. Fig. 8 presents the temperature variation along the central generatrix of the sharp cone during the experiment in accordance with the LC thermometry data. The inset in the right top corner shows the model before and in the run. The obtained data permit to obtain the estimations of the heat flux levels, but the comparison with the *a priory* data of IR and

calorimetric measurements has revealed that the LC data of the heat fluxes are underestimated.

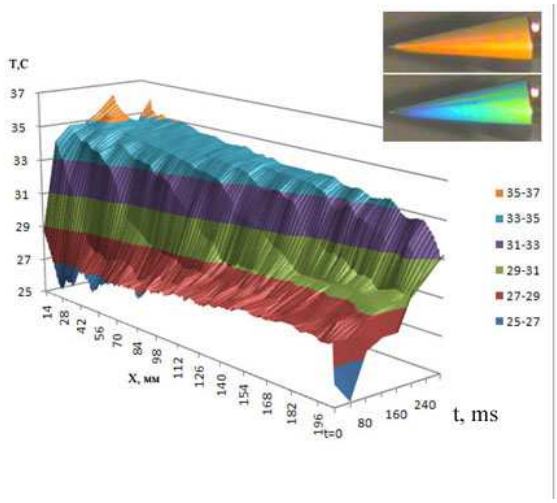

Fig. 8. Temperature variation along the central generatrix of the sharp cone during the experiment by the LC thermometry data. Inset in the right corner shows the model before and in the run. M = 10.9. The model is made of a thermal-insulating material.

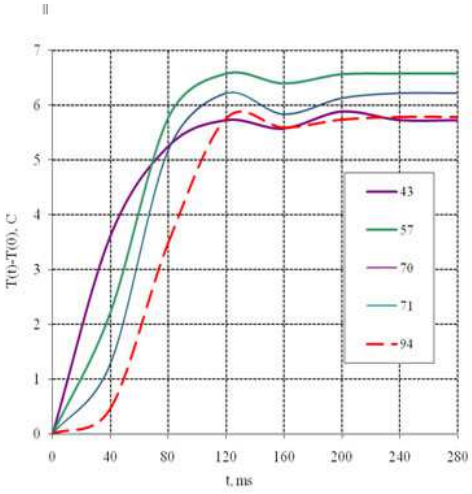

Fig. 9. Example of the temperature response of the LC to the step heat impulse in different points X along the central generatrix of the sharp cone at M = 10.9.

Method limitations. Fig. 9 presents the example of the LC response to the step heat impulse in various points X on the central generatrix of the sharp cone in a run at M = 10.9. Curves outlook make us presume that the LC indicator can be described by the transfer function of an oscillaing connection with a lag. Evident that as the regime duration is below 10 ms, the LC canoot be heated up to the assigned temperature value, hence the heat fluxes within this time will be underestimated as compared to the calorimetry data. If, in addition, the onset temperature in this run corresponds to the top boundary of the use LC working range (violet), the error will also occur in the measured onset temperature. This error can be avoided is the measurements are repeated when applying the LC of wider dynamic range, or two-range LC. Thus, in the short-duration hypersonic wind tunnels, when the experiment duration is below 100 ms, the main restriction of the LC indicators is related with their thermal inetria. As the experiment duration is longer and heat loads are high, the LC layer cannot be heated above the polymer melting point or LC evaporation point (≈100C).

7. VISUALIZATION AND MEASUREMENT OF SHEAR STRESS VECTOR

Regarding the initial orientation of molecules in the layer (LC texture), different effects are observed, which make the base for experimental procedures of shear stress measurement [18]. If the initial texture is confocal (Fig. 1), the effect of texture transition from the confocal into planar texture is used. Under the influence of the flow, the surface turns from colorless into colored one, and the LC response time depends on the shear stress level and direction.

If the initial texture is planar, we see the second effect of the light selective reflection by the planar texture. The dominating selective-reflection wave length λ_{max} depends on the shear level. In Fig. 10 an example of spectral response of SSLC on the multistep variation of flow velocity is shown in time. Color scale shows intensity level.

In order to obtain the quantitative data on the vector τ direction, the images must be registered in several azimuth positions. The azimuth (observation angle about the shift vector) effect is shown in Fig. 11. The method of τ visualization and measurement with the second effect is described in detail in the patent and works of Reda D.C. at all. [15].

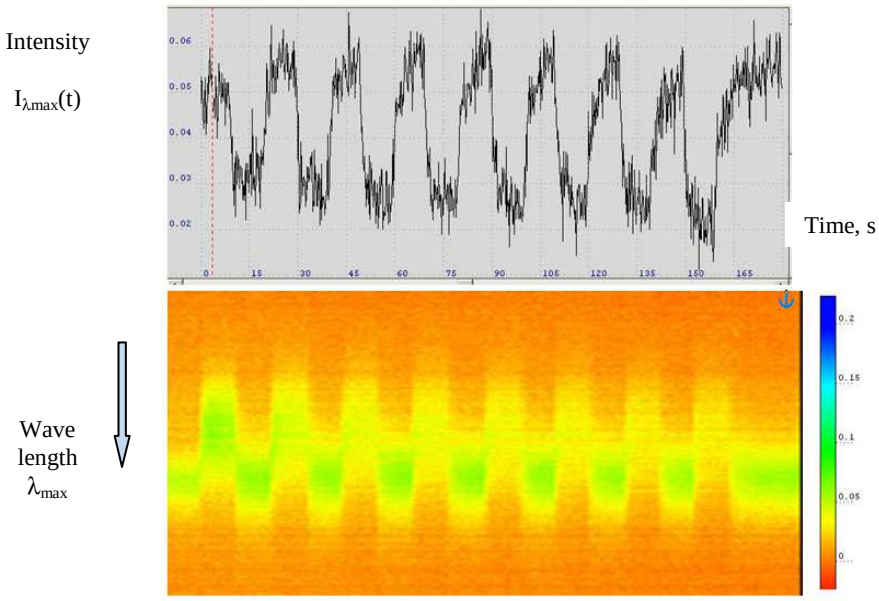

Fig.10. Variation of λmax(t) and $I_{\lambda max}(t)$.

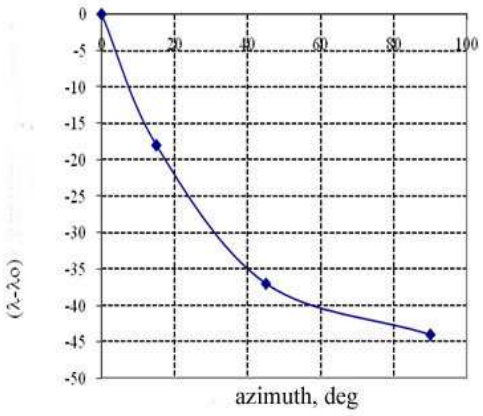

Fig. 11. Effect of the azimuth angle on the shift of the maximum wave length of the selective reflection (blue shift)

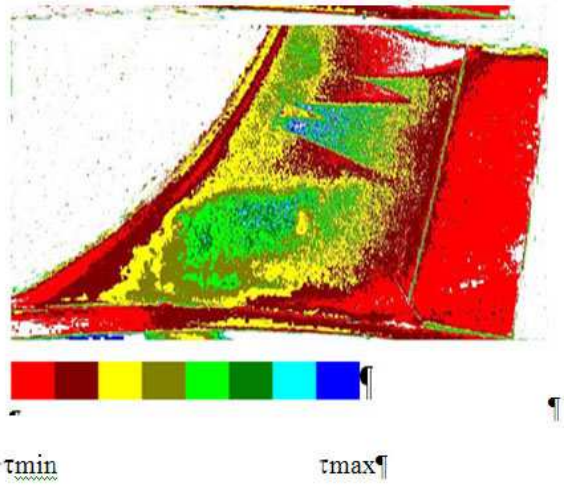

Fig. 12. Example of the shear stress distribution on the model surface at M = 0.2.

In ITAM, diagnostic LC compositions have been developed (binary and triple mixtures of cholesteric LCs), which are weakly sensitive to the temperature but sensitive to the shear stresses. Mechanical and optical properties of three-component ChLC compositions were studied. As the shear stress level is inreased, the LC color shifts toward the blue part of the visible spectrum [20]. Together with Central Aerohydrodynamic Institute (TsAGI), Zhukovsky, Russia, the developed LC mixtures, as well as the effect of selective light reflection by the planar ChLCs structure were experimentally tested in the transonic wind tunnel AT-128 TsAGI [21], the Mach numbers being from 0.2 to 0.9. The purpose of the tests was visualization of shear stress distribution on the vertical stabilizer of the model with turbulizers. Fig. 12 presents the map of the shear stresses obtained after the digital processing of the LC visualization data by the temperature-insensitive, shear-stress-sensitive LC indicators at M = 0.2. The areas of turbulent flow with increased levels of the tangential stress (green) are clearly seen in the wake behind the turbulizers and in the near-core area.

CONCLUSION

The paper presents a brief review of the properties of two kinds of LC indicators for temperature fields and shear stress diagnostics on the model surface. These indicators were tested in wide range of flow parameters. High –information panoramic data on heat-transfer and near-wall flow structure was obtained. In particular, LC coatings were used for temperature fields visualization on the models made of a thermal-insulating material at Mach numbers M = 10.9 and 14 in the short-duration hypersonic wind tunnel. Application of shear stress sensitive LCs on the metal model in industrial transonic wind tunnel at M = 0.2÷0.9 have demonstrated its feasibility for visualization of laminar-to-turbulent transition.

References

1. V.E. Mosharov, V.N. Radchenko. *Measurement of heat fluxes by means of luminescent temperature tranducers* //Proc. of TsAGI, 2007, T.XXXVIII, No 1-2, pp. 94-101.(in Russian)
2. Fonov V., Fonov S., Grants G., Crafton J. *Image processing technique for shear-stress optical measurements*.// 11th Int. symp. on flow visualization, 2004, University of Notre Dame. Indiana. USA.
3. Golubev M.P., Pavlov A.A. *Panoramic interference techniques for heat flux and surface pressure measurements*/XV Int. conf. on the methods of aerophysical research (ICMAR).Novosibirsk, Russia. 2010.
4. Klein E.J. *Liquid crystals in aerodynamic testing*. /Astronautics and Aeronautics 1968. No 6. pp. 70-73.
5. Klein E.J., Margozzi A.P. *Exploratory investigation of the measurement of skin friction by means of Liquid crystals* // Israel J. of Technology. 1969, V.7, No. 1-2, p. 173-180.
6. Zharkova G.M. *Optical phenomena in liquid crystals and their application in aerophysical studies.* LaserTechnology, V.32, N6, 2000.
7. Zharkova G.M., Kovrizhina V.N. *Panoramic diagnostics of surface temperatures and heat fluxes*./ IFZh (J. of Engineering Physics and Thermophysics). Vol. 83, No. 6. November-December 2010. (in Russian)
8. Zharkova G.M., Kovrizhina V.N., Petrov A.P., Smorodsky B.V., Knauss H., Roediger T., Wagner S., Kraemer E. *Comparative Heat Transfer Studies at Hypersonic Conditions by means of Three Measurement Techniques. Part I: Measurement Techniques, Experimental Setup and Preceding Investigations*./ Proc. of XIIIth Int. Conf. on the Methods of Aerophysical Research (ICMAR 2007) Pt I, Novosibirsk, Russia, pp.221-228.
9. Zharkova G.M., Kovrizhina V.N., Khachaturyan V.M. *A Study of the Flow Structure in the Near-wall Region of a Complex-chaped Channel using Liquid Crystals. - in Optical Methods and Data Processing in Heat and Fluid Flow*, Ed by C. Greated, J. Cosgrov, J.M. Buick, Trowbridge, UK, p. 143-150, 2002.
10. Zharkova G.M., Kovrizhina V.N., Khachaturyan V.M. *Liquid Crystal Thermography (LCT): State of the Art and Application in Aerodynamics*. 2nd European Conference for Aerospace Sciences (EUCASS-2007)
11. A.S. Sonin. *Introduction in liquid-crystal physics.* Moscow. Nauka.1983. (in Russian)
12. M. M. Gurevich. *Color and its measurement*, Moscow-Leningrad, 1950. (in Russian)
13. 13G.M. Zharkova. *Development of liquid-crystal thermography for heat-exchange tasks*. Doctoral Thesis. Novosibirsk, 1988. (in Russian)
14 G.M. Zharkova, A.S. Sonin. *Liquid-crystal composites*. Novosibirsk, Nauka, 1994. 214 p. (in Russian)
15 Reda D.C., Muratore J.J. *Measurement of surface shear stress vectors using liquid crystal coatings* AIAA J. 1994, 32, p.1576-82.
16 Sun J.H., Leong K.C., Liu C.Y. *Influence of hue origin on the hue-temperature calibration of thermochromic liquid crystals*.// Heat and mass transfer, 33 (1997) pp.121-127.
17 Kovrizhina V.N., Kharitonov A.M., Petrov A.P., Schpack S.I., Zharkova G.M., Zvegintsev V.I. //*The Study Of Hypersonic heat transfer by Liquid Crystals Thermography*. Proc.of the 6th European Symp. on Aerothermodynamics For Space Vechicles (EUCASS), 2008, Versailles, France.
18 Dismille P.J., Toy N. *Full Field Surface Shear Stress Measurements Using Liquid Crystals* /Report A332933, 1994.
19 US Patent 5 438 879, Reda D. C. *Method for measuring surface shear stress magnitude and direction using liquid crystal coatings*, 1995.
20 G.M. Zharkova, V.N. Kovrizhina, A.P. Petrov, R.A. Gordeev. *Experimental study of thin-film liquid-crystal coatings for panoramic diagnostics of tangential stress distribution over the model surface. Proc. of the 15th Int. Conf. On the Methods of Aerophysical Research (ICMAR).* Novosibirsk, Russia.2010. pp. 253-255.
21 Zharkova G.M., Kovrizhina V.N., A.P. Petrov A.P., Shapoval, E.S., Mosharov V.E. and Radchenko V.N. *Visualization of boundary layer transition by shear sensitive liquid crystals*.// Proc. Of PSFVIP-8: The 8th Pacific Symp. on Flow Visualization and Image Processing,- August 21st-25th, 2011 Moscow, Russia. No. 113. - P. 1-5. ISBN 978-5-8279-0093-1